



## OPEN Biochemical and structural characterization of a reactive intermediate deaminase A homolog from *Streptococcus sanguinis*

Alexa B. Benedict<sup>1,4</sup>, Adreana I. Aquino<sup>1</sup>, Brandi A. Buckner<sup>2</sup>, Swarmistha Devi Aribam<sup>3</sup>, Chhandosee Ganguly<sup>3</sup>, Leonard M. Thomas<sup>3</sup>, Philip Bourne<sup>3</sup>, Rakhi Rajan<sup>3</sup>, Diana M. Downs<sup>2</sup> & Vijayakumar Somalinga<sup>1</sup>✉

2-Aminoacrylate (2AA) is a short-lived enamine generated as a catalytic intermediate in the dehydration of serine by serine/threonine dehydratase enzymes. 2AA is a metabolic stressor capable of inactivating important pyridoxal phosphate dependent enzymes in a cell. Detoxification of 2AA in a cell is catalyzed by members of the Reactive intermediate deaminase (Rid) family of proteins, which is conserved across all domains of life. We recently identified a RidA homolog, SSA\_0809, hereafter SsRidA, in *Streptococcus sanguinis* with 50% protein sequence identity to a RidA from *Salmonella enterica*. 2AA deaminase activity assay revealed that SsRidA is capable of enzymatic deamination of 2AA to pyruvate. Furthermore, L-amino acid oxidase assays showed SsRidA has significant activity against several with imino-amino acids similar to the *S. enterica* RidA. In addition, functional complementation analysis found that SsRidA restored growth of *S. enterica ridA* mutant in minimal media constituted to increase 2AA stress in the cell. Finally, the crystal structure of SsRidA revealed a homotrimeric protein with active sites at the interface of two interacting monomers. Structure analysis also showed the presence of active site arginine residue along with an active site water molecule implicated in catalysis.

**Keywords** RidA, Enamine deaminase, *Streptococcus sanguinis*, 2-Amino acrylate, Metabolic stress

Identified in all domains of life, the YjgF/YER057c/UK114 family of proteins are highly conserved, low-molecular weight proteins with functions ranging from enamine/imine deaminase activity<sup>1–4</sup> to ribonuclease activity<sup>5</sup>. Based on phylogenetic and comparative genomic analyses, the YjgF/YER057c/UK114 family of proteins can be divided into nine subfamilies, RidA, Rid1–7, and RutC<sup>6,7</sup>. The nine Rid subfamilies can be further categorized into three groups, RidA, Rid1–3, and Rid4–7, based on the presence or absence of an essential arginine residue in the active site<sup>6,8</sup>. The RidA subfamily, which is typified by the presence of an essential arginine residue in the active site is one of the well-characterized members of the subfamilies<sup>3,6</sup>. Evidence for the role of RidA in deamination of enamine and/or imines was first demonstrated in *Salmonella enterica* by Lambrecht et al.<sup>1</sup>. This seminal work established that *S. enterica* RidA (previously YjgF) catalyzed the hydrolysis of the 2-aminocrotonate enamine/imine intermediate to 2-ketobutyrate and ammonia. This result led to its current designation as reactive intermediate/imine deaminase A (RidA)<sup>1</sup> to reflect its ability to hydrolyze short-lived imine/enamine intermediates generated by pyridoxal 5'-phosphate (PLP)-dependent enzymes. In the past decade, RidA homologs have been identified and biochemically characterized in a number of eukaryotic<sup>9,10</sup> and prokaryotic organisms<sup>11–14</sup>. Although several RidA homologs have been characterized, the mechanism of RidA activity is far from fully characterized due to the short half-life, reversible tautomerization, and the lack of robust detection methods for enamine/imine intermediates. Based on structural and site-directed mutagenesis studies,

<sup>1</sup>Department of Biological and Biomedical Sciences, Southwestern Oklahoma State University, Weatherford, OK, USA. <sup>2</sup>Department of Microbiology, University of Georgia, Athens, GA, USA. <sup>3</sup>Department of Chemistry and Biochemistry, University of Oklahoma, Norman, OK, USA. <sup>4</sup>Present address: The University of Oklahoma College of Medicine, Oklahoma City, OK, USA. ✉email: vijay.somalinga@swsu.edu

the proposed mechanism for RidA activity involves the nucleophilic attack of the enamine/imine substrate by active site water molecule resulting in the formation of keto acid product and ammonia as a byproduct<sup>2,15</sup>.

Structurally, all RidA proteins characterized to date share a common architecture exhibiting a barrel-shaped, homotrimeric organization with a central cavity<sup>16</sup>. RidA monomers are composed of 5 to 6 anti-parallel  $\beta$ -sheets with two  $\alpha$ -helices packed against the  $\beta$ -sheets. Active sites are formed at the interface of the interacting monomers with each RidA homotrimer displaying three active sites. The active site residues important for ligand binding and catalysis are contributed by both the interacting monomers. The RidA active site is composed of seven conserved invariant residues that are critical for substrate interaction<sup>17</sup>, active site water binding<sup>17</sup>, and catalysis<sup>18</sup>. Although RidA structure and active site architecture are relatively well-defined, the substrate specificity and role of active site residues other than the essential arginine residue remains obscure<sup>3</sup>. In addition, the physiological consequences of deleting *ridA* have shown to be organism specific<sup>3</sup>. Lack of *ridA* leads to motility defects in several bacteria including, *S. enterica*<sup>11</sup>, *Escherichia coli*<sup>11</sup>, *Pseudomonas aeruginosa*<sup>12</sup>, and *Campylobacter jejuni*<sup>13</sup>. Interestingly, the reason for the motility defects in *ridA* deficient *Campylobacter jejuni* is speculated to be due to defective protein glycosylation<sup>13</sup>, while in other bacteria regulation of flagellar genes seems to be an important factor<sup>11</sup>. Lack of a unified phenotype, and the negative effect of *ridA* deletion on the production of virulence factors emphasizes the need for the continued identification and characterization of RidA proteins in bacterial pathogens.

The human oral cavity is an ideal habitat for a plethora of microorganisms that thrive in this nutrient rich, moist, and warm environment<sup>19,20</sup>. One of the abundant group of bacteria that inhabits human oral cavity is the Viridans Group *Streptococci* (VGS)<sup>20</sup>. Genetically heterogeneous, VGS is grouped into at least 30 species<sup>21</sup>, commonly associated in a symbiotic interaction with its human host. Although considered harmless, in some cases, VGS can cause life-threatening infections in susceptible individuals<sup>21</sup>. *Streptococcus sanguinis* is a prominent member of VGS, and one of the leading causes of subacute infective endocarditis (SIE) in individuals with pre-existing cardiac anomalies<sup>22</sup>. In the past two decades, several groups have employed gene knock-out strategies to identify genes important for colonization and virulence in *S. sanguinis*<sup>23–26</sup>. These gene knock-out screens were successful in providing a global snapshot of genes essential for colonization and virulence, but questions remain regarding *S. sanguinis* pathometabolism (metabolic adaptation) during endocardial growth. Mutants of *ridA* in pathogens such as *S. enterica*, *P. aeruginosa*, and *C. jejuni* exhibit phenotypes associated with defective virulence factor production<sup>11–13</sup> and in *S. enterica* biochemical genetic analysis revealed that *ridA* mutants are defective in essential one-carbon (1C) metabolism<sup>27,28</sup>. The pleiotropic phenotypes observed in these organisms and the indirect role of RidA in 1C metabolism underlies the importance of identifying and characterizing this protein in other bacterial pathogens. In this study, we identified a RidA homolog, SSA\_0809 in *S. sanguinis* and demonstrated that SSA\_0809, henceforth known as SsRidA, has enamine deaminase activity. In addition, we establish that SsRidA is capable of neutralizing imine derivatives generated from a variety of L-amino acids. The in vivo activity of SsRidA was determined using a complementation test which showed that SsRidA in-trans can rescue the growth defects of *S. enterica ridA* mutants in minimal glucose media containing serine. In addition, we also solved the crystal structure of SsRidA at 2.0 Å resolution using X-ray crystallography and show that SsRidA is a homotrimer with three interfacial active sites similar to other well characterized RidA proteins.

## Materials and methods

### Bioinformatics

Protein homology search (BLASTp)<sup>29</sup> for the presence of RidA homologs in *S. sanguinis* was performed using *S. enterica RidA* and *C. jejuni* Cj1388 as queries against *S. sanguinis* genomic databases in KEGG (<https://www.genome.jp/kegg/>)<sup>30</sup>. The presence of a RidA domain in the newly identified homolog from *S. sanguinis* was ascertained using the conserved domain database (CDD; <https://www.ncbi.nlm.nih.gov/Structure/cdd/cdd.shtml>) prediction program. Multiple sequence alignment of newly identified SsRidA with RidA proteins from other organisms with structural data was performed using the multiple sequence alignment tool Clustal Omega (<https://www.ebi.ac.uk/Tools/msa/clustalo/>).

### Bacterial strains and growth condition

All the plasmids, primers and bacterial strains used in this study is listed in Table 1. Wild-type *E. coli* NEBa cells were routinely grown in trypticase soy broth (TSB) media at 37 °C with shaking at 200 revolutions per minute (rpm) and supplemented with 35  $\mu$ g/mL kanamycin when necessary for plasmid maintenance. The expression host, *E. coli* BL21(DE3) was purchased from Novagen (USA) and high-density cultures of *E. coli* BL21(DE3) for protein purification were grown either in Terrific broth or in Super broth with 35  $\mu$ g/mL kanamycin. *Salmonella enterica* serovar Typhimurium LT2 was routinely maintained in Difco nutrient broth (8 g/L) with NaCl (5 g/L) or nutrient agar containing 15 g/L Difco BiTek agar. Growth assays were performed using no-carbon E (NCE) minimal media supplemented with 1 mM MgSO<sub>4</sub><sup>31</sup>, trace minerals (0.1X)<sup>32</sup> and 11 mM glucose. The amino acids isoleucine and serine were used at 1 mM and 5 mM respectively where indicated. Antibiotics, ampicillin (15  $\mu$ g/mL in minimal medium and 150  $\mu$ g/mL in rich medium) and kanamycin (50  $\mu$ g/mL), were used for selection or plasmid maintenance where necessary.

### Growth experiments

Growth experiments to assess the function of SsRidA in vivo were performed with modifications as reported in Irons et al.<sup>13</sup>. Briefly, *S. enterica* cultures were obtained by inoculating single colonies into 1 ml Difco nutrient broth supplemented with ampicillin. Cultures were incubated at 37 °C with shaking for 16–24 h before being pelleted and resuspended in an equal volume of sterile 0.85% NaCl. Experiment was performed in biological triplicate. The resulting cell suspension was used to inoculate sterile NCE minimal media (1% inoculum, 200  $\mu$ l

Strains		
Strain number	Genotype	Source
<i>E. coli</i> strains		
	NEB alpha/pET28a-SsRidA	Somalinga lab
-	NEB alpha	Somalinga lab
-	BL21(DE3)/pET28a-SsRidA	Somalinga lab
-	BL21-AI	Downs lab
-	BL21-AI/pET28a-SsRidA	This study
-	DH5 $\alpha$	Downs lab
DM17353	DH5 $\alpha$ /pET28a-SsRidA	This study
DM14502	DH5 $\alpha$ /pCV1	Downs lab
DM17375	DH5 $\alpha$ /pCV1-SsRidA	This study
<i>Salmonella enterica</i> LT2 strains		
DM15418	WT/pCV1	Downs lab
DM15419	ridA3::Mud/pCV1	Downs lab
DM15421	ridA3::Mud/pCV1-SeRidA	Downs lab
DM17376	ridA3::Mud/pCV1-SsRidA	This study

**Table 1.** Bacterial strains and plasmids used in this study.

final volume) in a 96 well microtiter plate. The microtiter plate was sealed with parafilm. Growth was monitored for 24 h at 37 °C under shaking conditions using a BioTek ELx808 microtiter plate reader. The data obtained by monitoring bacterial growth at OD<sub>650nm</sub> was plotted using GraphPad Prism 9.0 (GraphPad software, CA, USA).

### Molecular biology

The gene encoding for SsRidA was codon-optimized for *E. coli* expression and synthesized by Genscript (NJ, USA). SsRidA gene codon optimized for *E. coli* expression was digested out of the pUC57 plasmid using NdeI and XhoI restriction endonucleases. The digested gene was gel-purified using Qiagen gel extraction kit (Qiagen, MD) and ligated to pET28a vector previously digested with the same set of restriction endonucleases. Ligation was performed at 16 °C overnight using T4 DNA ligase (NEB, USA). Ligations were transformed into *E. coli* NEB $\alpha$  (NEB, USA) competent cells for propagation. Plasmids were purified from the transformants and were sequenced (Oklahoma Medical Research Foundation, OK, USA) to confirm the presence of *S. sanguinis* *ridA* gene.

Modified pCV1 plasmid<sup>33</sup> carrying the full-length *S. sanguinis* *ridA* gene was constructed using a BspQI-based cloning method as described in<sup>34</sup>. Briefly, codon-optimized *S. sanguinis* *ridA* was PCR-amplified from pET28a-SsRidA using Q5 Polymerase (New England Biolabs) and primers encoding BspQI restriction sites. The resulting PCR product and the empty pCV1 vector were digested using BspQI, and then ligated together using Fast-Link Ligase (Lucigen, USA). Plasmid was sequence-verified by sequencing (Eurofins Genomics, USA).

### Protein overexpression, production and purification

Overexpression of SsRidA for crystallization was performed by transforming the recombinant pET28a plasmid containing *ssridA* gene into *E. coli* BL21(DE3) expression host. The transformants were then inoculated in LB (Luria Bertani) broth containing kanamycin (35  $\mu$ g/mL) and grown over-night at 37 °C with shaking (200 rpm). The overnight cultures were then transferred to 500 mL of Terrific broth supplemented with 35  $\mu$ g/mL of kanamycin, and grown at 37 °C with shaking (200 rpm), until an OD<sub>600nm</sub> of 0.6 was reached for each culture. This was followed by overnight induction with 0.5 mM IPTG (Isopropoyl- $\beta$ -D-thiogalactopyranoside) at 20 °C. Cells were then harvested by centrifugation (10,000 RPM, 10 min at 4 °C) and the cell pellets were stored at -20 °C until use. SsRidA purification for crystallization was performed using gravity-based method. Overexpressed cell pellet was resuspended in buffer A (20 mM Tris pH 7.5, 500 mM NaCl, and 30 mM imidazole), and the cells were lysed by sonication on ice. SsRidA purification was carried out according to Somalinga et al.<sup>35</sup>. Eluted SsRidA was dialyzed against buffer containing 20 mM Tris pH 7.5, 150 mM NaCl over-night at 4 °C. Additional purification of SsRidA was carried out using Hiprep 16/60 Sephacryl S-200 (GE healthcare, Pittsburgh, PA) gel-filtration column. Purified SsRidA was concentrated to ~10.6 mg/mL using Amicon centrifugal filter, molecular weight cut-off (MWCO) 10 kDa (Millipore), for SsRidA crystallization.

Overexpression of SsRidA for biochemical assay was carried out according to Ernst et al.<sup>36</sup>. Briefly, overnight culture of *E. coli* BL21AI strain containing pET28a-SsRidA was inoculated into 1.5 L of Super Broth (SB) containing 50  $\mu$ g/mL kanamycin and incubated at 37 °C with shaking (150 RPM). When the culture reached an OD<sub>650nm</sub> of 0.7–0.8, expression of SsRidA was induced with the addition of 0.2% arabinose and 0.5 mM IPTG (final concentrations). Upon induction, temperature was lowered to 30 °C and the culture was incubated overnight with shaking. Cells were harvested by centrifugation and the cell pellets were stored at -80 °C until use. Cells were resuspended in binding buffer (50 mM potassium phosphate buffer (pH 8.0), 100 mM NaCl, 10% glycerol, 20 mM imidazole) and treated with 1 mg/mL lysozyme, 20 U/mL DNase and 1 mM PMSF. Resuspended cells were lysed at 18 Kpsi using a One-Shot Cell Disruptor (Constant Systems, USA). The cell lysate was centrifuged at 40,000  $\times$  g for 45 min at 4 °C and the cleared supernatant was filtered using a 0.45- $\mu$ m

syringe filter to remove fine cell debris. Filtered supernatant was loaded on to a 5 mL Nickel-Sepharose HisTrap HP column (Cytvia, MA) that was pre-equilibrated with the binding buffer. SsRidA was then eluted with elution buffer (50 mM potassium phosphate buffer pH 8.0, 100 mM NaCl, 10% glycerol, and 500 mM imidazole) with a linear gradient of imidazole (20 to 500 mM imidazole). The purified SsRidA protein was dialyzed in 7000 MWCO SnakeSkin dialysis tubing (Thermo Scientific, USA) overnight at 4 °C against dialysis buffer (50 mM potassium phosphate buffer pH 8.0, 100 mM NaCl, 10% glycerol). Protein was concentrated to ~20 mg/mL using an Amicon Ultra-15 centrifugal filter (MWCO 10 kDa, Millipore, MA). The concentrated protein was flash-frozen dropwise in liquid nitrogen and stored at -80 °C until use.

### 2-Aminoacrylate deaminase assay

An assay for the ability of Rid proteins to deaminate 2AA generated by cysteine desulfurase (CdsH) was performed as reported in Ernst et al.<sup>36</sup>. CdsH protein was previously purified as reported. CdsH assay reaction mixture contained 0.25 mM NADH, 30  $\mu$ M pyridoxal phosphate (PLP), 5 U per reaction lactate dehydrogenase in 100 mM Tris-HCl (pH 8.0). SsRidA or *S. enterica* RidA (SeRidA) and CdsH were added to the reaction mixture at a final concentration of 0.27  $\mu$ M and 0.19  $\mu$ M respectively. Reactions (300  $\mu$ L) were performed in a quartz 96 well plate and initiated with the addition of varying concentrations (0–2 mM) of fresh L-cysteine stock. Plates were shaken for 5 s before 1st read. The reactions were continuously monitored at 22 °C using a Spectramax 384 Plus microplate reader (Molecular Devices, USA) to measure the absorbance at 340 nm. The rate of pyruvate formation was calculated using Beer's law, the extinction coefficient of NADH at 340 nm (6220 M<sup>-1</sup> cm<sup>-1</sup>), and the change in absorbance from 0 to 30 s. All experiments were performed in triplicate, and the data was plotted using GraphPad Prism 9 (GraphPad software, CA, USA).

### Imino-acid deaminase assay

The ability of Rid proteins to deaminate various imino acids was assayed using an L-amino acid oxidase (LOX)-based assay as reported in<sup>8,13</sup> with modification. The LOX assay mixture contained 50 mM potassium pyrophosphate (50 mM, pH 8.7), neutralized semicarbazide (10 mM), bovine liver catalase (1  $\mu$ g/ $\mu$ L), *Crotalus adamanteus* LOX (0.5  $\mu$ g/ $\mu$ L), and 10  $\mu$ M SsRidA or SeRidA. Assay was initiated with the addition of 10  $\mu$ M L-amino acid substrates (L-leucine, L-glutamine, L-phenylalanine, L-methionine or L-histidine). To measure semicarbazone formation, the absorbance at 248 nm was measured every 10 s for 10 min using a Spectramax 384 Plus microplate reader (Molecular Devices). Rate of semicarbazone formation was determined using Beer's law and the molar extinction coefficient of semicarbazone at 248 nm (10,300 M<sup>-1</sup> cm<sup>-1</sup>). Each 100  $\mu$ L reaction was performed in duplicate in a quartz 96 well plate.

### Crystallization, data collection and refinement of SsRidA

Crystallization screens for SsRidA were set-up in 96-well crystallization plates using vapor diffusion sitting-drop method. Purified SsRidA at 10.6 mg/mL was mixed with 0.3  $\mu$ L of crystallization screen conditions (0.3  $\mu$ L protein solution + 0.3  $\mu$ L crystallization condition) using a Mosquito liquid handling system (SPT Labtech). Crystallization conditions identified using the preliminary sparse matrix screen were used for optimization screens. Numerous small crystals formed after a few days in Midwest Center for Structural Genomics 2 (MCSG 2) Crystal Screen 2 containing 24% w/v PEG 1500, 20% glycerol. The crystal was harvested and flash frozen in a nitrogen stream and diffraction data were collected. Crystallographic data for SsRidA were collected in house using a Rigaku MicroMax 007HF microfocuss X-ray generator equipped with VariMax HF optics coupled to a Dectris Pilatus P200K silicon hybrid pixel detector. The data were collected at 100 K with CuK $\alpha$  radiation ( $\lambda$  = 1.54178 Å) with the generator operation at 1200 kV. Data were indexed and integrated using HKL3000R<sup>37</sup>. The data was scaled in space group C 1 2 1, with unit cell parameters of a = 168.5 Å, b = 61.8 Å, c = 75.7 Å and  $\alpha$  =  $\gamma$  = 90°,  $\beta$  = 113.4°. The structure of SsRidA was solved by molecular replacement using PHASER<sup>38</sup>. The search model was a RidA homolog from *Streptococcus mutans* (PDB ID: 3L7Q), which has 88% sequence identity with SsRidA. Refinement and model building of the resultant structure were done using phenix.refine<sup>39</sup> and COOT<sup>40</sup>. The model has an  $R_{work}$  = 0.201 and  $R_{free}$  = 0.260. Data and refinement statistics for SsRidA is summarized in Table 2. Visualization of protein crystal structures were performed using PyMol molecular graphics program<sup>41</sup>.

### SsRidA oligomerization status analysis using SEC-MALS

Oligomerization status of SsRidA was analyzed using size-exclusion chromatography with multiangle light scattering (SEC-MALS). Running buffers for all the SEC-MALS runs is composed of 20 mM Tris, pH 7.5 and 150 mM NaCl. The freshly purified protein was dialyzed overnight at 4 °C and concentrated to 10 mg/mL. The protein was further diluted to 1.0 mg/mL, 6.5 mg/mL and 7.0 mg/mL with the running buffer. Bovine Serum Albumin (BSA) dissolved at a concentration of 5 mg/mL in running buffer was used as reference. One hundred  $\mu$ L of each sample (dilutions) was injected onto a Superdex 200 Increase column 10/300 GL (GE) with an inline miniDAWN TREOS (Wyatt Technology Co.) multiangle light scattering detector and Optilab T-rEX (Wyatt Technology Co.) differential refractometer. Molar mass analysis was carried out using ASTRA (version 7.3.0) software (Wyatt Technology Co.).

## Results and discussion

### Identification and sequence analysis of Ssa0809 (SsRidA) in *S. sanguinis*

The presence of a RidA homolog in the genome of *S. sanguinis* was identified by BLASTp<sup>29</sup> sequence similarity search analysis. Using Cj1388, a characterized RidA protein from *Campylobacter jejuni* as a query sequence, we mined the genome of *S. sanguinis* SK36 for homologs which resulted in the retrieval of a single protein with 57% identity to Cj1388. The newly identified RidA homolog from *S. sanguinis* with a locus tag Ssa0809 is an ~ 15 kDa protein that is annotated as putative translation initiation inhibitor, YjgF family/endoribonuclease L-PSP.

Wavelength (Å)	1.54178
Resolution range (Å)	34.75–2.004 (2.05–2.0)
Space group	C 1 2 1
Unit cell (Å)(°)	168.5 61.8 75.7 90.0 113.4 90.0
Total reflections	291,545
Unique reflections	47,652 (3089)
Multiplicity	6.1 (2.7)
Completeness (%)	98.86 (90.03)
Mean I/sigma(I)	9.10 (1.17)
Wilson B-factor	31.39
$R_{\text{meas}}$	0.125 (1.073)
$R_{\text{pim}}$	0.046 (0.619)
CC1/2	0.870 (0.493)
Reflections used in refinement	47,652 (3089)
Reflections used for R-free	1990 (122)
$R_{\text{work}}$	0.2014 (0.3084)
$R_{\text{free}}$	0.2601 (0.3358)
Number of non-hydrogen atoms	6114
macromolecules	5683
solvent	431
Protein residues	749
RMS(bonds)	0.002
RMS(angles)	0.47
Ramachandran favored (%)	97.29
Ramachandran allowed (%)	2.71
Ramachandran outliers (%)	0
Rotamer outliers (%)	0.49
Clashscore	3.58
Average B-factor	36.78
macromolecules	36.49
solvent	40.48

**Table 2.** Data and refinement statistics for SsRidA.

Although annotated as translation initiation inhibitor/endoribonuclease, the high level of sequence similarity of the newly identified protein from *S. sanguinis* suggests that Ssa0809 may represent an uncharacterized RidA homolog. The newly identified Ssa0809 was further characterized using Clustal Omega multiple sequence alignment program<sup>42</sup> which revealed the presence of the seven invariant residues typical of Rid family of proteins (SI Fig. S1). In addition, multiple sequence analysis also showed the presence of a critical arginine residue, which is typical of RidA subfamily, in Ssa0809 (SI Fig. S1)<sup>6</sup>. These seven invariant residues including the arginine residue form the active site of RidA family of proteins have been shown to be essential for deamination since the substitution of these residues completely abolishes activity<sup>1</sup>. The presence of seven conserved invariant residues including the important arginine residue in Ssa0809 indicates that this protein may represent a newly identified RidA in *S. sanguinis*.

### SsRidA catalyzes the conversion of 2-aminoacrylate (2AA) to pyruvate in-vitro

Sequence analysis and conserved domain search clearly showed the presence of conserved invariant and catalytically important arginine residue in SsRidA (SI Fig. 1) indicating that this protein may have the ability to neutralize toxic 2AA intermediates. To test SsRidA's ability to hydrolyze 2AA to pyruvate, a coupled assay using cysteine desulfhydrase (CdsH) and lactate dehydrogenase was performed. In this assay, CdsH generates 2AA from cysteine. 2AA can spontaneously hydrolyze to form pyruvate, but functional 2AA deaminases, such as RidA from *S. enterica*, can rapidly catalyze this conversion to pyruvate. Thus, addition of RidA proteins significantly increases the rate of pyruvate formation compared the rate of spontaneous hydrolysis. In the presence of SsRidA, the rate of pyruvate formation increased in a concentration dependent manner, reaching maximal conversion at 5 mM of L-cysteine (Fig. 1). The rate of pyruvate formation catalyzed by SsRidA was similar to the positive control, SeRidA (Fig. 1), a well-characterized RidA protein from *S. enterica*<sup>1,36</sup>.

The cysteine desulfhydrase (CdsH) assay is well-established and indirectly measures the rate of pyruvate formation via 2AA intermediate by coupling it to NADH oxidation by lactate dehydrogenase<sup>13,36,43</sup>. The 2AA intermediate is either spontaneously or enzymatically hydrolyzed to pyruvate. The enzymatic hydrolysis of 2AA to pyruvate is catalyzed by RidA and the enzymatic hydrolysis proceeds at a faster rate compared to spontaneous hydrolysis<sup>1,36</sup>.

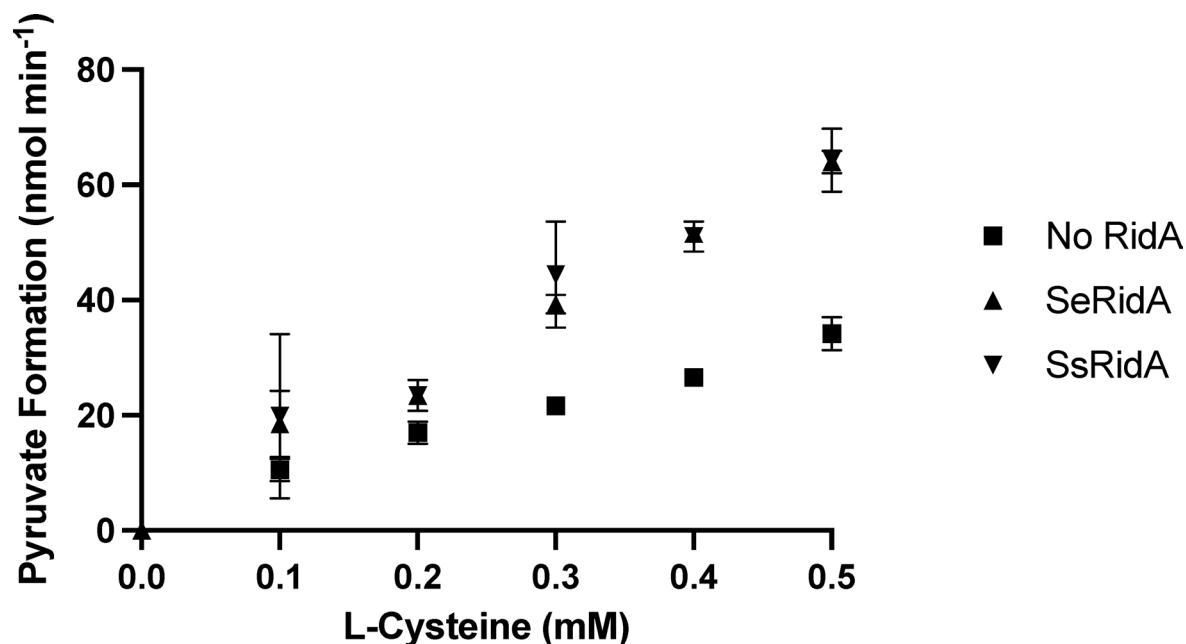


**Fig. 1.** SsRidA has 2AA deaminase activity in vitro. Increased pyruvate formation in reactions containing SsRidA indicates that SsRidA is capable of catalyzing 2AA deamination. Each coupled assay contained NADH (0.25 mM), PLP (30  $\mu$ M), 5LDH (5 U per 300  $\mu$ l reaction), and CdsH (0.19  $\mu$ M) in 100 mM Tris-HCl (pH 8.0). RidA proteins (SeRidA or SsRidA) were present at 0.27  $\mu$ M when indicated. Reactions were performed in triplicate in a 96-well quartz plate and were initiated with addition of L-cysteine at varying concentrations. The plate was shaken for 5 s before first read. The rate of pyruvate formation was calculated using Beer's law, the extinction coefficient of NADH (6220  $M^{-1} cm^{-1}$ ), and the absorbance at 340 nm from 0 to 30 s. Graph was constructed in Prism 9 (GraphPad). Error bars represent standard deviation.

Amino acid metabolism is an essential process in all living organisms and proceeds via oxidative or non-oxidative deamination of amino acids. Deamination of certain amino acids, specifically  $\alpha$ -amino acids with electronegative sidechains such as serine, cysteine etc., proceeds via the formation of reactive, short-lived intermediates that can be non-enzymically converted to ketoacids<sup>2</sup>. Enzymes that catalyze these reactions have the fold of type II PLP-dependent  $\alpha,\beta$ -eliminases such as serine/threonine dehydratase or CdsH that convert amino acids to a keto acid and ammonia via enamine intermediates<sup>1,2,36</sup>. The reaction catalyzed by CdsH is a prototypical  $\alpha$ -eliminase reaction that results in the formation of pyruvate and ammonia via an 2AA enamine intermediate<sup>43</sup>. Hydrolysis of the 2AA to pyruvate occurs spontaneously or enzymatically, catalyzed by RidA<sup>13,36,43</sup>. In our CdsH assay, the rate of pyruvate formation was  $\sim$ twofold higher in the presence of SsRidA, indicating the protein had accelerated the rate of enamine hydrolysis to pyruvate (Fig. 1). Furthermore, the rate of pyruvate formation catalyzed by SsRidA was similar to the control reaction catalyzed by a well-characterized RidA from *S. enterica*<sup>36</sup>. This result clearly demonstrates that SsRidA is an imine/enamine deaminase from *S. sanguinis*.

### SsRidA is capable of neutralizing amino acid derived imino intermediates in-vitro

In addition to neutralizing 2AA, RidA is capable of hydrolyzing imines derived from amino acid catabolism<sup>6,8,13</sup>. The ability of SsRidA to catalyze the hydrolysis of imines was assessed using an established L-amino acid oxidase (LOX) assay<sup>8,13</sup>. The LOX assay utilizes *Crotalus adamanteus* venom-derived, FAD-dependent L-amino oxidase to generate imines from amino acid substrates. The imines produced are derivatized using semicarbazide to produce semicarbazone which can be measured using a spectrophotometer at 248 nm<sup>6</sup>. The rate at which semicarbazone is produced is inversely proportional to the RidA activity.

Imines generated from five different amino acids (L-methionine, L-glutamine, L-histidine, L-arginine, and L-phenylalanine) using LOX were used as substrates to test the imine deaminase activity of SsRidA. Compared to control reactions performed in the absence of RidA protein, reactions containing SsRidA exhibited significant reduction in semicarbazone formation in all tested amino acids except for arginine, indicating that this newly identified enzyme is capable of catalyzing the deamination of amino acid derived imines (Fig. 2). The amount of semicarbazone formed in reactions containing SsRidA were  $\sim$  4.5-fold,  $\sim$  3.5-fold,  $\sim$  onefold, and  $\sim$  1.5-fold lower with L-methionine, L-glutamine, L-histidine, and L-phenylalanine as substrates respectively, while reaction containing L-arginine as substrate did not show any significant decrease in semicarbazone formation. These results indicate SsRidA can utilize all amino acid derived imines tested, other than the L-arginine derived imine, as substrates (Fig. 2). The imine deaminase activity of SsRidA was compared with the activity of SeRidA, a well-characterized reactive intermediate deaminase from *S. enterica*<sup>1</sup>. Similar to SsRidA, SeRidA was capable of imine deamination, but interesting differences were seen between the catalytic ability of SsRidA and SeRidA

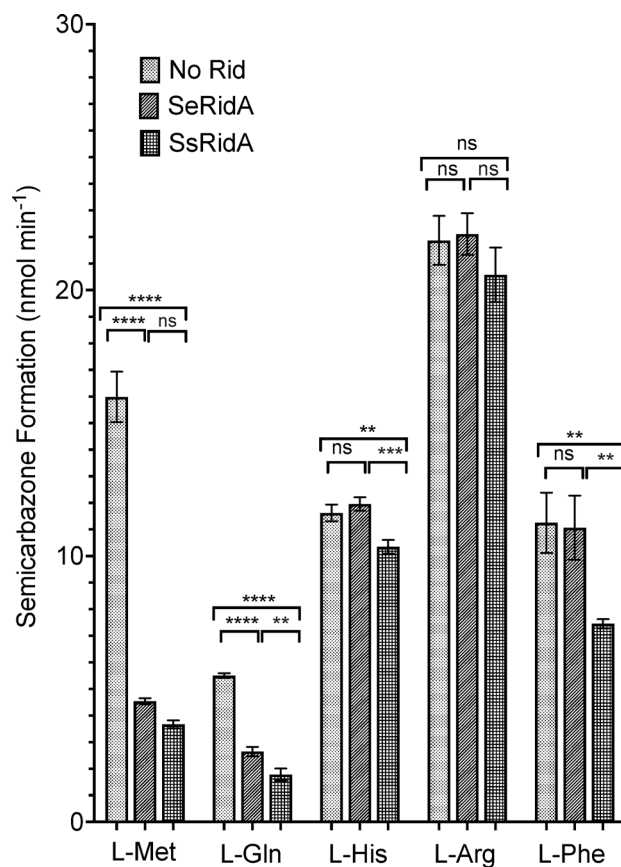


**Fig. 2.** SsRidA displays imino acid deaminase activity *in vitro*. Each coupled assay contained 50 mM potassium pyrophosphate buffer (pH 8.7), neutralized semicarbazide (100 mM), bovine liver catalase (1  $\mu\text{g}/\mu\text{L}$ ), and *C. adamanteus* L-amino acid oxidase (LOX) (0.5  $\mu\text{g}/\mu\text{L}$ ), 10  $\mu\text{M}$  RidA protein when indicated, and 10  $\mu\text{M}$  L-amino acids (L-methionine, L-glutamine, L-histidine, L-arginine, or L-phenylalanine). Reactions were performed in duplicate in a 96-well quartz plate and were initiated with the addition of 10  $\mu\text{M}$  indicated L-amino acid. The plate was shaken for 5 s before first read and absorbance of semicarbazone was measured for 10 min at 248 nm. Graph was constructed in Prism 9 (GraphPad). Error bars represent standard deviation. Significance of this assay was determined using Student's t test. Asterisk indicates statistical significance ( $p < 0.05$ ) while ns indicates not significant.

(Fig. 2). Two amino acids (L-histidine, and L-arginine) with positively charged side chains, one amino acid (L-glutamine) with negatively charged side chain, one amino acid (L-methionine) with nonpolar side chain, and one amino acid (L-phenylalanine) with aromatic side chain were selected for this study based on the reactivity of various amino acid derived imines with RidA. Niehaus et al.<sup>6</sup> demonstrated that amino acids with polar, charged side chains such as L-arginine, L-histidine etc. served as poor substrates for SeRidA. Furthermore, the same study determined that amino acids with non-charged side chains such as methionine served as ideal substrates for SeRidA. Our work here reconfirms these findings and establishes that SsRidA exhibits preference for imines with non-charged side chains, while amino acids with polar, charged side chains remained poor substrates (Fig. 2). Similarly, amino acid with non-charged side chains (L-methionine), served as an ideal substrate for SsRidA as indicated by a very significant (~3.6-fold) reduction in semicarbazone formation.

### ***S. sanguinis ridA* is capable of restoring growth in *S. enterica* mutant lacking *ridA***

The role of RidA in neutralizing enamine intermediates generated by serine/threonine dehydratase during amino acid biosynthesis was first demonstrated in *S. enterica*<sup>18</sup>. In minimal media containing serine, *S. enterica ridA* mutant failed to grow due to 2AA toxicity, and this phenotype was rescued by providing *ridA in-trans*<sup>18</sup>. Recently, a *C. jejuni ridA* provided *in trans* to a *S. enterica ridA* mutant was able to rescue the growth of the mutant in serine-supplemented minimal media indicating the role of RidA in neutralizing toxic intermediates generated during amino acid metabolism<sup>13</sup>. The CdsH and LOX assays (Figs. 1, 2) demonstrated the ability of SsRidA to deaminate imine/enamine intermediates to non-toxic by-products *in-vitro*. To ascertain the *in vivo* activity of SsRidA, the gene encoding for SsRidA was cloned into a pBAD24 based vector, pCV1, under the control of an arabinose-inducible promoter. The resulting pCV1 vector containing *S. sanguinis ridA* or the empty vector was transformed into a *S. enterica ridA* mutant. In minimal media containing glucose as a carbon source, no significant difference in the growth rates were observed for wild-type *S. enterica* carrying empty pCV1 vector or *ridA* mutants containing pCV1 vector or pCV1 encoding *S. enterica ridA* or *S. sanguinis ridA* designated

as pSeRidA and pSsRidA respectively (Fig. 3A). Upon supplementation of serine, *S. enterica ridA* mutants harboring empty vector fail to grow while the wild-type *S. enterica* grow to full density (Fig. 3B). The serine sensitivity exhibited by the *S. enterica ridA* mutant is complemented by expression of either *S. enterica ridA* or *S. sanguinis ridA* in trans (Fig. 3B). Complementation of the *ridA* mutant can be achieved without arabinose-induction of plasmid-encoded *ridA* genes—indicating that low level expression of SsRidA or SeRidA is sufficient for complementation. As expected, the growth defect observed in the *S. enterica ridA* mutant containing empty pCV1 vector in serine-containing media is restored to wild-type levels of growth with addition of isoleucine (Fig. 3C).

The physiological role of RidA was first described in *S. enterica* when a *ridA* mutant was sensitive to exogenous serine supplementation<sup>3</sup>. The sensitivity to serine was due to the catalytic activity of PLP-dependent serine/threonine dehydratase which generates 2AA as an intermediate when acting upon serine as a substrate<sup>18</sup>. Serine sensitivity phenotype of *S. enterica* was rescued by the addition of isoleucine, an allosteric inhibitor of serine/threonine dehydratase (IlvA), establishing the role of IlvA as one of the prime generators of 2AA in *S. enterica*<sup>44</sup>. The same mechanism of serine-dependent enamine generation was also observed in other organisms such as *Saccharomyces cerevisiae*<sup>45</sup> and *Arabidopsis thaliana*<sup>9</sup>. Interestingly, in a recent study in *C. jejuni*<sup>13</sup>, it was determined that IlvA was not the major contributor of toxic enamine intermediates indicating the presence of other enamine generators in this pathogen. The diversity of metabolic and phenotypic perturbations observed in response to *ridA* inactivation points to organism-specific impacts necessitating a thorough examination of RidA's role in each organism.

### SsRidA exhibits a conserved chorismate mutase-like fold and a homotrimer organization

The structure of SsRidA in apoenzyme conformation was solved at 2.0 Å resolution by molecular replacement method using the structure of *S. mutans* RidA (PDB ID:3L7Q) as a template. Monomeric SsRidA is ~15 kDa protein made up of 126 amino acid residues folded into a six stranded β-sheet with β-strands 5 and 6 in parallel orientation while other four β-sheets are in an antiparallel orientation (Fig. 4A). Similar to other well-

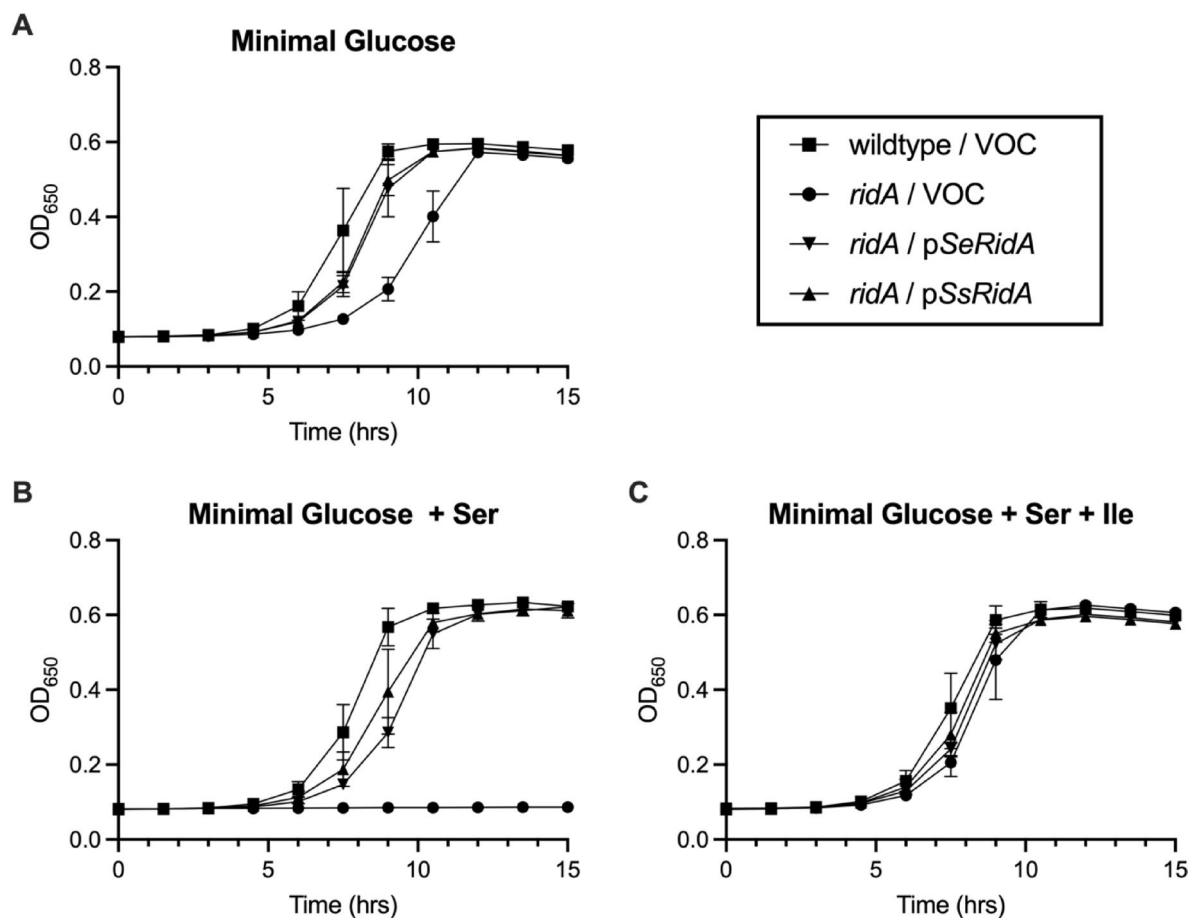


**Fig. 3.** SsRidA rescues serine sensitivity of *Salmonella enterica ridA* mutant. *S. enterica ridA* mutants harboring one of three plasmids were grown at 37 °C in a 96-well plate with shaking in (A) minimal glucose media, (B) minimal glucose media with serine (5 mM), or (C) serine and isoleucine. The *S. enterica* wild type carrying empty vector only control (squares) (VOC), or *S. enterica ridA* mutant harboring empty vector (circles), *S. enterica ridA* (pSeRidA) (inverted triangles) or *S. sanguinis ridA* (pSsRidA) (triangles). Graph was constructed in Prism 10 (GraphPad). Error bars represent standard deviation.

characterized RidA monomers, the loops connecting  $\beta$ -strands are long and meandering on one side (bottom in the orientation shown in Fig. 4A), while the other side (top in the orientation shown in Fig. 4A) is short. The chorismate mutase-like fold conserved in RidA protein family has been described in detail elsewhere<sup>46</sup>.

Analogous to other well-characterized RidA homologs, SsRidA monomers organize into a homotrimer both in crystal and in solution. The core of the trimer is composed of 15  $\beta$ -sheets contributed by each interacting monomer resulting in a closed, barrel-like structure with the 6  $\alpha$ -helices packed around the central core forming the periphery of the SsRidA trimer (Fig. 4B). Size exclusion chromatography-multi angle light scattering (SEC-MALS) analysis of SsRidA revealed a calculated average mass of  $43.5 \pm 0.3\%$  kDa indicating a homotrimeric organization (SI Fig. 2). SsRidA's tertiary and quaternary structure is analogous to other well-studied RidA proteins from prokaryotes<sup>17,46</sup> and eukaryotes<sup>16,47</sup>.

### SsRidA active site analysis reveals catalytically essential arginine residue and active site water molecules

The active site of all RidA proteins is formed at the interface of two interacting monomers<sup>16,17,46,47</sup>. The interfacial clefts formed between subunit pairs are solvent-accessible and may represent the active site of SsRidA. The amino acids that form the active site of RidA is composed of 7 invariant residues that play important roles in substrate binding and catalysis<sup>6,18</sup>. Site directed mutagenesis studies of these invariant residues in *S. enterica* RidA have revealed that only Arg105 is essential for catalysis<sup>18</sup>. Mutagenesis of other invariant residues such as Tyr16 and Glu120 in *S. enterica* RidA, although resulted in decreased RidA activity, did not completely abolish its catalytic activity<sup>15,18</sup>. All the 7 invariant residues (Tyr17, Gly31, Asn57, Asn89, Arg103, Pro112 and Glu118; residue numbering of SsRidA) including the catalytically essential Arg residue is present in SsRidA (Fig. 5). Similar to other characterized RidA proteins, these residues are contributed by both the monomers (Fig. 5). The organization of invariant residues in the active site of SsRidA indicates that the catalytic mechanism may mirror other described RidA proteins including the *S. enterica* RidA. The catalytic mechanism of RidA from *S. enterica*, was proposed to involve the active site residues Arg105 forming a bidentate salt bridge with the carboxylate of the substrate, while Tyr17 forms a hydrogen bond with the imine nitrogen of the iminobutyrate substrate<sup>18</sup>. This interaction helps in orienting and stabilizing the substrate for nucleophilic attack by the active site water molecule held in position by hydrogen bond networks via Cys107 and Glu120 residues. The resulting nucleophilic attack on the C2 of the imine substrate results in the formation of 2-ketobutyrate and ammonia<sup>18</sup>. Superimposition of the active site invariant residues of SsRidA with *E. coli* YjgF (PDB ID: 1QU9)<sup>46</sup> and *E. coli* TdcF (PDB ID: 2UYK)<sup>17</sup> reveals a high degree of positional and orientational conservation of these residues indicating that SsRidA (Fig. 5) may employ a similar catalytic mechanism. Furthermore, active site analysis of SsRidA also reveals the presence of a cluster of active site water molecules (SI Fig. 3) reported in other RidA homologs<sup>17,46</sup> with one of the active site waters in the vicinity of the catalytically important Arg103 residue (SI Fig. 3). In *S. enterica* RidA, the water molecule positioned near catalytically important arginine residue is implicated in catalysis and shown to be located  $\sim 2.0$  Å from the C2 for the active site substrate molecule<sup>18</sup>. The proximity of active site water to catalytically important arginine residue, the conservation of active site amino

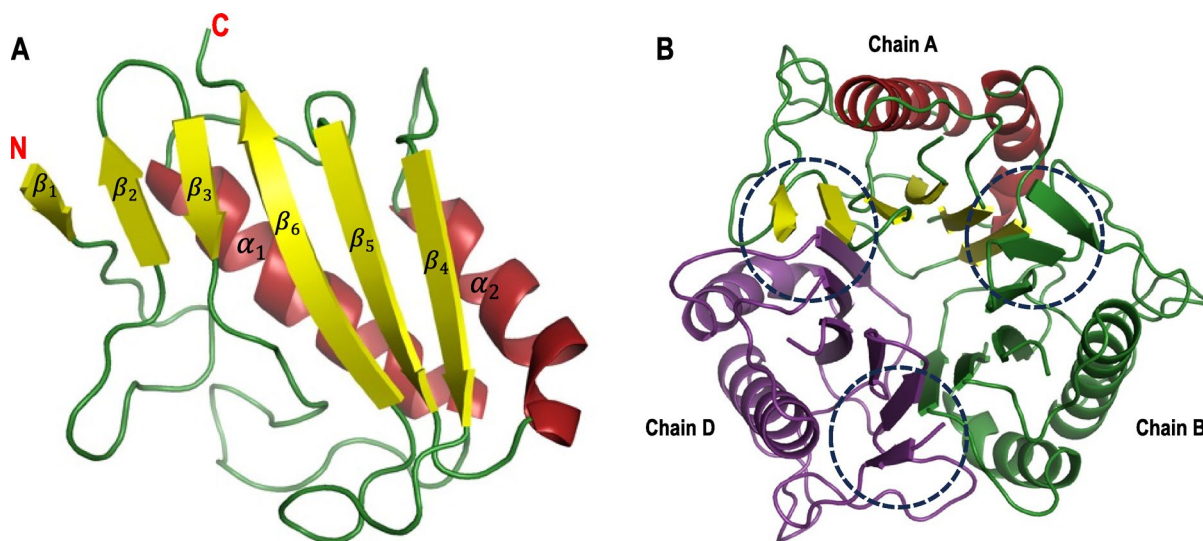


**Fig. 4.** Overall structure of SsRidA. **(A)** Cartoon representation of SsRidA monomer structure. The monomer core is composed of two  $\alpha$ -helices (red) packed against a mixed beta sheet consisting of six  $\beta$ -strands (yellow) and the loops connecting the  $\alpha$ -helices and  $\beta$ -strands are shown in green. **(B)** Cartoon representation of overall structure of SsRidA homotrimer with active sites shown within dashed circles. Individual interacting monomers of SsRidA homotrimer is colored independently. Chain A was used as representative of SsRidA monomer structure. SsRidA cartoon representation was created using PyMol molecular graphics program, version 2.5.5; Schrödinger LLC (<https://www.pymol.org/>)<sup>41</sup> with ray tracing set at mode 2.

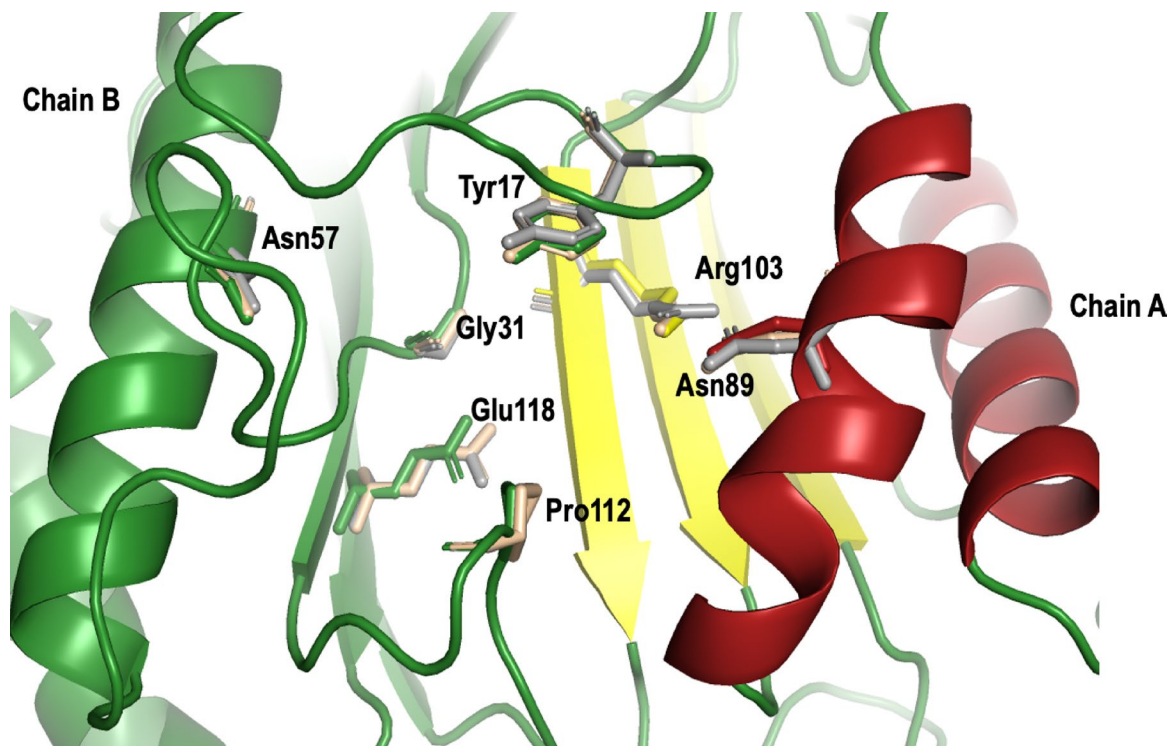


**Fig. 5.** Comparison of the active site of SsRidA with its homolog from *E. coli*. Superposition of SsRidA active site with active sites from 1QU9 (grey) and 2UYK (wheat) showing the geometry of 7 invariant residues. Active site residues contributed from two adjacent chains, Asn89 and Arg103 from chain A and Tyr17, Gly31, Asn57, Pro112 and Glu118 from chain B are clearly visible in this structure. SsRidA is represented as cartoon structure and follows the same color coding seen in Figs. 1A,B. Active site invariant residues (numbering based on SsRidA) are represented as sticks and the active site residues of SsRidA follows the same color coding of respective chains. Root mean square deviation (RMSD) values between SsRidA (Chain A) and its *E. coli* homologs 1QU9 (Chain A) and 2UYK (Chain A) are 0.96 and 0.92 respectively for 124 aligned residues. SsRidA cartoon and active site residue stick representations were created using PyMol molecular graphics program, version 2.5.5; Schrödinger LLC (<https://www.pymol.org/>)<sup>41</sup> with ray tracing set at mode 2. RMSD values were calculated using RCSB pairwise structural alignment tool.

acids, and the structural and oligomeric similarities indicate that SsRidA may adopt a catalytic mechanism similar to other characterized RidA proteins. (<https://www.pymol.org/>)<sup>41</sup>

## Conclusions

The work presented in this manuscript was initiated to understand the structure and function of SsRidA, an important protein that plays a critical role in detoxifying at least one metabolic intermediate in both prokaryotes and eukaryotes. Biochemical characterization of SsRidA revealed that this protein is capable of catalyzing hydrolytic deamination of imine/enamine intermediates and demonstrated unique substrate specificity profiles. In addition, structural characterization of SsRidA showed monomeric and oligomeric organization that is typical of the members of RidA protein family. Furthermore, the conservation and organization of active site residues indicate that the catalytic mechanism of SsRidA may be similar to the mechanism proposed for other members in the RidA family. Although some of the fundamental questions about the structure and function of SsRidA have been answered in this paper, questions remain about the substrate preference, specificity, catalytic mechanism and the physiological roles of SsRidA. Efforts are underway in our laboratory to address these important questions about the nature of this protein and its role in the physiology of *S. sanguinis*.

## Data availability

The SsRidA structure described in this manuscript has been deposited in the protein databank (<https://www.rcsb.org/>) and the PDB ID is 8V8R. All the strains, protocols, and materials outlined in this work will be available upon request. The structure of SsRidA (SSA\_0809) was deposited as PDB ID: 8V8R.

Received: 10 December 2024; Accepted: 2 June 2025

Published online: 01 July 2025

## References

- Lambrecht, J. A., Flynn, J. M. & Downs, D. M. Conserved YjgF protein family deaminates reactive enamine/imine intermediates of pyridoxal 5'-phosphate (PLP)-dependent enzyme reactions. *J. Biol. Chem.* **287**(5), 3454–3461 (2012).
- Borchert, A. J., Ernst, D. C. & Downs, D. M. Reactive imines and enamines in vivo: Lessons from RidA paradigm. *Trends Biochem. Sci.* **44**(10), 849–860. <https://doi.org/10.1016/j.tibs.2019.04.011> (2019).
- Irons, J. L., Gerdes, S., Hodge-Hanson, K. & Downs, D. M. RidA proteins protect against metabolic damage by reactive intermediates. *Microbiol. Mol. Biol. Rev.* **84**(3), e00024–e120 (2020).
- Fulton, R. L. & Downs, D. M. Modulators of a robust and efficient metabolic metabolism: Perspectives and insights from the Rid superfamily of proteins. *Adv. Microb. Physiol.* **83**, 117–179 (2023).
- Morishita, R. et al. Ribonuclease activity of rat liver perchloric acid-soluble protein, a potent inhibitor of protein synthesis. *J. Biol. Chem.* **274**(29), 20688–20692 (1999).
- Niehaus, T. D. et al. Genomic and experimental evidence for multiple metabolic functions in the RidA/YjgF/YER057c/UK114(Rid) protein family. *BMC Genom.* **16**, 382. <https://doi.org/10.1186/s12864-015-1584-3> (2015).
- Buckner, B. A., Lato, A. M., Campagna, S. R. & Downs, D. M. The Rid family member RutC of *Escherichia coli* is a 3-aminoacrylate deaminase. *J. Biol. Chem.* **296**, 100651 (2021).
- Hodge-Hanson, K. & Downs, D. M. Members of the Rid protein family have broad imine deaminase activity and can accelerate the *Pseudomonas aeruginosa* D-arginine dehydrogenase (DauA) reaction in vitro. *PLoS ONE* **12**(9), e0185544 (2017).
- Niehaus, T. D. et al. Arabidopsis and maize RidA proteins preempt reactive enamine/imine damage to branched-chain amino acid biosynthesis in plastids. *Plant Cell* **26**, 3010–3022 (2014).
- ElRamlawy, K. G. et al. Der f 34, a novel major house dust mite allergen belonging to a highly conserved Rid/YjgF/YER057c/UK114 family of imine deaminases. *J. Biol. Chem.* **291**(41), 21607–21615 (2016).
- Borchert, A. J. & Downs, D. M. The response to 2-aminoacrylate differs in *Escherichia coli* and *Salmonella enterica*, despite shared metabolic components. *J. Bacteriol.* **199**, e00140–e217 (2017).
- Irons, J., Hodge-Hanson, K. M. & Downs, D. M. PA5339, a RidA homolog is required for full growth in *Pseudomonas aeruginosa*. *J. Bacteriol.* **200**, e00434–e518 (2018).
- Irons, J., Sacher, J. C., Szymanski, C. M. & Downs, D. M. Cj1388 is a RidA homolog and is required for flagella biosynthesis and/or function in *Campylobacter jejuni*. *Front. Microbiol.* **10**, 2058 (2019).
- Martinez-Chavarria, L. C. et al. Putative horizontally acquired genes, highly transcribed during *Yersinia pestis* flea infection, are induced by hyperosmotic stress and function in aromatic amino acid metabolism. *J. Bacteriol.* **202**, e00733–e819 (2020).
- Downs, D. M. & Ernst, D. C. From microbiology to cancer biology: The Rid protein family prevents cellular damage caused by endogenously generated reactive nitrogen species. *Mol. Microbiol.* **96**(2), 211–219 (2015).
- Xie, L., Zeng, J., Chen, X. & Xie, W. Crystal structures of RidA, an important enzyme for the prevention of toxic side products. *Sci. Rep.* **6**, 30494. <https://doi.org/10.1038/srep30494> (2016).
- Burman, J. D., Stevenson, C. E., Sawers, R. G. & Lawson, D. M. The crystal structure of *Escherichia coli* TdcF, a member of the highly conserved YjgF/YER057c/UK114 family. *BMC Struct. Biol.* **7**(30), 1–14 (2007).
- Lambrecht, J. A., Schmitz, G. E. & Downs, D. M. RidA proteins prevent metabolic damage inflicted by PLP-dependent dehydratases in all domains of life. *MBio* **4**(1), e00033–e113. <https://doi.org/10.1128/mBio.00033-13> (2013).
- Baker, J. L., Mark Welch, J. L., Kaufmann, K. M., McLean, J. S. & He, X. The oral microbiome: Diversity, biogeography and human health. *Nat. Rev. Microbiol.* **22**(2), 89–104. <https://doi.org/10.1038/s41579-023-00963-6> (2024).
- Sedghi, L., DiMassa, V., Harrington, A., Lynch, S. V. & Kapila, Y. L. The oral microbiome: Role of key organisms and complex networks in oral health and disease. *Periodontol.* **2000**(87), 107–131 (2021).
- Doern, C. D. & Burnham, C. D. It's not easy being green: The viridans group *Streptococci*, with a focus on pediatric clinical manifestations. *J. Clin. Microbiol.* **48**(11), 3829–3835 (2010).
- Holland, T. L. et al. Infective endocarditis. *Nat. Rev. Dis. Primers* **2**, 1–22 (2016).
- Paik, S. et al. Identification of virulence determinants of endocarditis in *Streptococcus sanguinis* by signature-tagged mutagenesis. *Infect. Immun.* **73**(9), 6064–6074 (2005).
- Ge, X. et al. Identification of *Streptococcus sanguinis* genes required for biofilm formation and examination of their role in endocarditis virulence. *Infect. Immun.* **76**(6), 2551–2559 (2008).
- Crump, K. E. et al. The relationship of the lipoprotein SsaB, manganese and superoxide dismutase in *Streptococcus sanguinis* virulence for endocarditis. *Mol. Microbiol.* **92**(6), 1243–1259 (2014).
- Martini, A. M. et al. Association of novel *Streptococcus sanguinis* virulence factors with pathogenesis in a native valve infective endocarditis model. *Front. Microbiol.* **11**, 10. <https://doi.org/10.3389/fmicb.2020.00010> (2020).
- Flynn, J. M., Christopherson, M. R. & Downs, D. M. Decreased coenzyme A levels in *ridA* mutant strains of *Salmonella enterica* result from inactivated serine hydroxymethyltransferase. *Mol. Microbiol.* **89**(4), 751–759 (2013).
- Ernst, D. C., Anderson, M. E. & Downs, D. M. L-2,3-diaminopropionate generates diverse metabolic stresses in *Salmonella enterica*. *Mol. Microbiol.* **101**(2), 210–223 (2016).
- Camacho, C. et al. BLAST+: Architecture and applications. *BMC Bioinform.* **15**(10), 421. <https://doi.org/10.1186/1471-2105-10-421> (2009).
- Kanehisa, M., Furumichi, M., Sato, Y., Matsuura, S. & Ishiguro-Watanabe, M. KEGG: Biological systems database as a model of the real world. *Nucleic Acids Res.* **53**, D672–D677. <https://doi.org/10.1093/nar/gkac909> (2025).
- Vogel, H. J. & Bonner, D. M. Acetylornithinase of *Escherichia coli*: partial purification and some properties. *J. Biol. Chem.* **218**, 91–106 (1956).
- Balch, W. E. & Wolfe, R. S. New approach to the cultivation of methanogenic bacteria: 2-mercaptoethanesulfonic acid (HS-CoM)-dependent growth of *Methanobacterium ruminantium* in a preussurized atmosphere. *Appl. Environ. Microbiol.* **32**, 781–791. <https://doi.org/10.1021/cg400171z> (1976).
- VanDrise, C. M. & Escalante-Semerena, J. C. New high-cloning-efficiency vectors for complementation studies and recombinant protein overproduction in *Escherichia coli* and *Salmonella enterica*. *Plasmid* **86**, 1–6. <https://doi.org/10.1016/j.plasmid.2016.05.001> (2016).
- Galloway, N. R., Toutkoushian, H., Nune, M., Bose, N. & Momany, C. Rapid cloning for protein crystallography using type IIS restriction enzymes. *Cryst. Growth Des.* **13**, 2833–2839 (2013).
- Somalinga, V., Foss, E. & Grunden, A. M. Biochemical characterization of a psychrophilic and halotolerant alpha-carbonic anhydrase from a deep-sea bacterium, *Photobacterium profundum*. *AIMS Microbiol.* **9**(3), 540–553. <https://doi.org/10.3934/microbiol.202328> (2023).
- Ernst, D. C., Lambrecht, J. A., Schomer, R. A. & Downs, D. M. Endogenous synthesis of 2-aminoacrylate contributes to cysteine sensitivity in *Salmonella enterica*. *J. Bacteriol.* **196**(18), 3335–3342 (2014).
- Minor, W., Cymborowski, M., Otwinowski, Z. & Chruszcz, M. HKL-3000: The integration of data reduction and structure solution—From diffraction images to an initial model in minutes. *Acta Crystallogr. D Biol. Crystallogr.* **62**, 859–866 (2006).
- McCoy, A. J. et al. Phaser crystallographic software. *J. Appl. Crystallogr.* **40**, 658–674 (2007).
- Liebschner, D. et al. Macromolecular structure determination using X-rays, neutrons and electrons: Recent developments in Phenix. *Acta Cryst.* **D75**, 861–877 (2019).
- Emsley, P., Lohkamp, B., Scott, W. & Cowtan, K. Features and development of coot. *Acta Crystallogr. D Biol. Crystallogr.* **66**(4), 486–501 (2019).

41. DeLano, W. L. PyMOL: An open-source molecular graphics tool. *Protein Crystallogr.* **1**, 82–92 (2002).
42. Sievers, F. et al. Fast, scalable generation of high-quality protein multiple sequence alignments using clustal Omega. *Mol. Syst. Biol.* **7**, 539. <https://doi.org/10.1038/msb.2011.75> (2011).
43. Kredich, N. M., Foote, L. J. & Keenan, B. S. The stoichiometry and kinetics of inducible cysteine desulfhydrase from *Salmonella typhimurium*. *J. Biol. Chem.* **248**, 6187–6196 (1973).
44. Schmitz, G. E. & Downs, D. M. Reduced transaminase B (IlvE) activity caused by the lack of *yjgF* is dependent on the status of the ornithine decarboxylase (IlvA) in *Salmonella enterica* serovar Typhimurium. *J. Bacteriol.* **186**(3), 803–810 (2004).
45. Ernst, D. C. & Downs, D. M. Mmf1p couples amino acid metabolism to mitochondrial DNA maintenance in *Saccharomyces cerevisiae*. *MBio* **9**, e84–e18. <https://doi.org/10.1128/mBio.00084-18> (2018).
46. Volz, K. A test case for structure-based functional assignment: the 1.2 Å crystal structure of the *yjgF* gene product from *Escherichia coli*. *Protein Sci.* **8**, 2428–2437 (1999).
47. Digiovanni, S. et al. Two novel fish paralogs provides insights into the Rid family of imine deaminases active in pre-empting enamine/imine metabolic damage. *Sci. Rep.* **10**, 10135. <https://doi.org/10.1038/s41598-020-66663-w> (2020).

## Acknowledgements

This work was supported by IDeA-NIGMS-NIH award under grant # P30GM145423 awarded to Vijay Somalinga and Rakhi Rajan. This work was also supported by the OK-INBRE SMART award, OK-LSAMP, SWOSU Guy Hagin Endowment fund and SWOSU CAS grants awarded to the students involved in the project and Vijay Somalinga. A part of this project was also supported by National Science Foundation grant, DBI-1757720. This work was also supported by funding from the NIH to D.M.D (GM095837) and B.A.B (1T32GM142623). This work also acknowledges the help and support provided by the Biomolecular Structure Core, The University of Oklahoma, Norman, Protein Production and Characterization Core, The University of Oklahoma, Norman, Office of Sponsored Programs, SWOSU and the Department of Biological and Biomedical Sciences, SWOSU.

## Author contributions

VS designed the overall study and supervised the project. DD and BB designed and supervised SsRidA biochemical characterization. VS and RR designed and supervised SsRidA structural characterization. AB, AA and BB were involved in SsRidA purification and biochemical characterization. CG and PB performed SEC-MALS studies. LT solved the crystal structure of SsRidA. SA, LT, RR and VS were involved in SsRidA structure analysis. VS wrote the manuscript. All authors were involved in manuscript review and editing. All authors approved this final submission.

## Declarations

### Competing interests

The authors declare no competing interests.

### Additional information

**Supplementary Information** The online version contains supplementary material available at <https://doi.org/10.1038/s41598-025-05264-x>.

**Correspondence** and requests for materials should be addressed to V.S.

**Reprints and permissions information** is available at [www.nature.com/reprints](http://www.nature.com/reprints).

**Publisher's note** Springer Nature remains neutral with regard to jurisdictional claims in published maps and institutional affiliations.

**Open Access** This article is licensed under a Creative Commons Attribution-NonCommercial-NoDerivatives 4.0 International License, which permits any non-commercial use, sharing, distribution and reproduction in any medium or format, as long as you give appropriate credit to the original author(s) and the source, provide a link to the Creative Commons licence, and indicate if you modified the licensed material. You do not have permission under this licence to share adapted material derived from this article or parts of it. The images or other third party material in this article are included in the article's Creative Commons licence, unless indicated otherwise in a credit line to the material. If material is not included in the article's Creative Commons licence and your intended use is not permitted by statutory regulation or exceeds the permitted use, you will need to obtain permission directly from the copyright holder. To view a copy of this licence, visit <http://creativecommons.org/licenses/by-nc-nd/4.0/>.

© The Author(s) 2025